Available online at www.sciencedirect.com
SCIENCE DIRECT®
Cement and Concrete Research 36 (2006) 364 – 370
Cement and Concrete Research

Investigation of the structure of ettringite by time-of-flight neutron powder diffraction techniques

M.R. Hartman *, R. Berliner

University of Michigan, Ann Arbor, MI 48109, USA

Received 29 September 2004; accepted 22 August 2005

Abstract

The crystalline structure of ettringite, $Ca_6[Al(OH)_6]_2(SO_4)_3 \cdot \sim 26H_2O$, was investigated using high-resolution time-of-flight neutron powder diffraction techniques. The powder diffraction data were subjected to Rietveld crystal structure refinement. The resultant ettringite crystal structure confirmed the positions of Ca, Al, and S atoms while permitting a more precise determination of the locations of O and H atomic positions than in previous X-ray and neutron diffraction studies. A discussion of the ettringite hydrogen bonding network is presented, illustrating the role of hydrogen bonding in the stabilization of the ettringite structure.

Keywords: Crystal structure; Neutron powder diffraction; Physical properties; Calcium aluminate cement; Ettringite

1. Introduction

Ettringite, $Ca_6[Al(OH)_6]_2(SO_4)_3 \cdot \sim 26H_2O$, is an important mineral in the chemistry of cement at two very different time scales. During the early hydration stages of Portland cements, the formation of ettringite is important for controlling the rate of set of the highly reactive calcium aluminate phase, $Ca_3Al_2O_6$ [1]. At the other temporal extreme, an understanding of ettringite is necessary to describe the destructive processes in mature cement pastes arising from sulfate attack [2] and delayed ettringite formation [3]. The crystalline structure of ettringite has been previously investigated by Berliner [4] using neutron powder diffraction techniques with a reactor-based instrument. Berliner's crystalline structural model consisted of a central column of aluminum and calcium coordination polyhedra with surrounding columns of sulfate tetrahedra and rigid water molecules in the P 3 1 *c* space group with $a = 1.11670(5)$ nm and $c = 2.13603(13)$ nm. Recent investigations into the formation of ettringite concomitant with the hydration of the calcium aluminate phase in the presence of gypsum, as well as a study of the structural changes during the thermal decomposition of ettringite, using time-of-flight (TOF) neutron powder diffraction [5] revealed that the presently accepted description of the ettringite crystalline structure [4] was inadequate. To resolve the discrepancies in the structural model, phase-pure ettringite was synthesized and subjected to structural investigation using TOF neutron powder diffraction techniques.

TOF neutron diffraction employs a pulsed neutron beam from an accelerator driven neutron source. Neutrons diffracted from the specimen are captured in an array of detectors that simultaneously record the scattering angle and flight time of the scattered neutron. These two quantities allow the momentum transfer of the scattering process to be determined. Pulsed neutron diffraction instruments provide improved instrumental resolution at large momentum transfers or, equivalently, small d-spacings.

2. Experimental

2.1. Ettringite synthesis

Two different synthesis methods were employed. Boiled deionized H_2O and D_2O were used in both synthesis methods to preclude the incorporation of impurity ions into the ettringite structure. Additionally, the syntheses were conducted in a sealed

* Corresponding author. National Institute of Standards and Technology, 100 Bureau Drive, MS 8562, Gaithersburg, MD 20899-8562, USA.
E-mail address: michael.hartman@nist.gov (M.R. Hartman).

0008-8846/$ - see front matter © 2005 Elsevier Ltd. All rights reserved.
doi:10.1016/j.cemconres.2005.08.004

glove box with an inert nitrogen atmosphere to eliminate the influence of CO_2 on the reactions.

In the first method, denoted as Struble's method [6], ettringite was synthesized by dissolving 0.06749 moles of $Ca(OH)_2$ in 400 cc of a 10 wt.% sucrose solution in H_2O. A separate solution of 0.01125 moles of $Al_2(SO_4)_3{\cdot}18H_2O$ in 50 cc of H_2O was also prepared. After magnetically stirring both solutions, they were combined and stirred further to ensure proper mixing of the reactants. The ettringite precipitate was vacuum-filtered and rinsed with H_2O several times to remove any sucrose or unreacted material. Following the final rinse, the ettringite was vacuum-filtered and allowed to dry over a saturated solution of LiCl (11% RH) in H_2O.

Ettringite obtained by Struble's method was crushed to a fine powder and was characterized using X-ray diffraction, scanning electron microscopy (SEM), and thermogravimetric analysis (TGA). X-ray diffraction analysis of the ettringite showed the material to be nearly phase-pure with a trace amount of calcite but no indications of residual $Ca(OH)_2$ or $Al_2(SO_4)_3{\cdot}18H_2O$. SEM revealed acicular crystals characteristic of the ettringite crystalline habit [7]. TGA exhibited weight-loss curves similar to those reported by other researchers [4,7]. For neutron powder diffraction examination, it is necessary to substitute deuterium for hydrogen in the ettringite structure to eliminate the large incoherent scattering background signal that would otherwise be present due to the hydrogen. Attempts to deuterate the ettringite by soaking it in D_2O for a period of several weeks proved unsuccessful, as evidenced by preliminary neutron scattering measurements.

To overcome the difficulties in producing a well-deuterated ettringite encountered with Struble's method, a second synthesis method, denoted as direct-synthesis, was employed. The direct-synthesis method eliminated the use of sucrose and used D_2O in lieu of H_2O. $Ca(OH)_2$, contaminated with trace amounts of calcite, was heated for a period of 24 h at 1000 °C, resulting in pure CaO. The CaO was reacted with D_2O, forming a moist $Ca(OD)_2$ paste which was subsequently dried over a saturated solution of LiCl in D_2O. The dried $Ca(OD)_2$ was crushed into a fine powder and characterized using X-ray powder diffraction. The ettringite synthesis then proceeded by creating one solution of 0.07884 moles of $Ca(OD)_2$ in 650 cc of D_2O and another consisting of 0.01314 moles of anhydrous aluminum sulfate, $Al_2(SO_4)_3$, in 150 cc of D_2O. The two solutions were both magnetically stirred to ensure proper mixing. The aluminum sulfate solution was added to the $Ca(OD)_2$ solution and the resultant mixture was magnetically stirred for a period of 24 h. The ettringite precipitate was vacuum-filtered and dried over a saturated solution of LiCl in D_2O.

Ettringite obtained by the direct-synthesis method was crushed into a fine powder and subjected to X-ray diffraction, SEM, and TGA investigations. In contrast to the sample obtained by Struble's method, X-ray diffraction showed a phase-pure ettringite with no visible traces of calcite or other phases. SEM indicated an acicular crystalline habit, shown in Fig. 1, characteristic of ettringite [7]. The deuterated ettringite was subjected to neutron powder diffraction and exhibited a reduced background signal and a much improved signal-to-noise ratio.

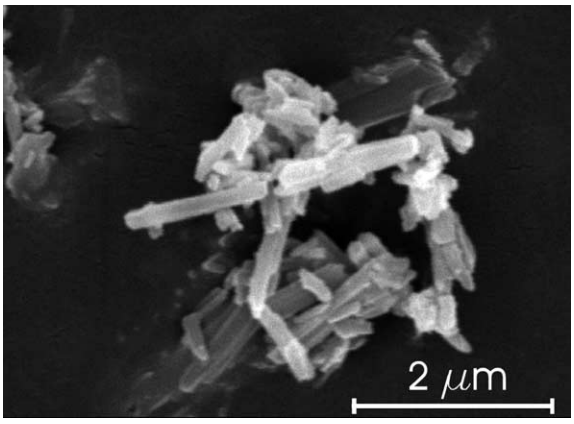

Fig. 1. SEM photograph of deuterated ettringite from the direct-synthesis method, demonstrating acicular crystalline habit.

2.2. TOF neutron powder diffraction

The direct-synthesis ettringite was investigated using the Special Environment Powder Diffractometer (SEPD) [8] at the Intense Pulsed Neutron Source (IPNS) at Argonne National Laboratory by placing the finely crushed ettringite powder into a vanadium sample can under a helium atmosphere. Once sealed, the sample can was placed in the instrument and data were collected at a temperature of 10 K. Data acquisition at low temperature minimizes the thermal motion of the atoms, permitting a precise determination of their equilibrium positions. The data acquisition exposed the sample to the neutron beam for a period of approximately 20 h to obtain data of sufficient statistical quality for Rietveld crystal structure refinement.

3. Discussion

3.1. Rietveld crystal structure refinement

The neutron powder diffraction data were subjected to Rietveld crystal structure refinement [9], denoted hereafter as structural refinement, using the *GSAS* [10] computer code as implemented in *EXPGUI* [11]. The structural refinement employs a non-linear least-squares fitting of a crystalline structural model to the diffraction data. The structural model is modified and compared to the data in an iterative fashion until close agreement between the model and the data is achieved. A detailed description of the Rietveld crystal structure refinement method is given by Young [12]. The initial positions for all atoms were taken to be those of Berliner's structural refinement [4]. The ettringite utilized for the experiment had deuterium in place of hydrogen, however in the discussion that follows, those sites that contain deuterium or hydrogen will be generically referred to as hydrogen sites for notational convenience. Initially, soft restraints, which apply stereochemical restrictions to the motions of atoms, were applied to the hydroxyl, water, and sulfate molecules. Soft restraints permit variation of a parameter, such as a bond length or bond angle, about a nominal or expected value but prevent non-physical distortions of known molecular identities within a crystal

structure. Attempts to refine a restrained parameter away from the statistical distribution defined for the parameter results in the application of a penalty in the refinement process. The magnitude of the penalty is determined by a user defined weighting function in conjunction with the normalized deviance of the restrained parameter from its nominal value. The hydroxyls were restrained to have a bond length of 0.0960±0.0005 nm (Note: deviance is quoted as one-sigma standard deviation). Water molecules were restrained to have the nominal configuration of free water with an O–H bond length of 0.0980±0.0005 nm and an H–O–H angle of 104.5°±5.0°. Sulfate tetrahedra were restrained to have S–O bond lengths of 0.149±0.005 nm and O–S–O bond angles of 109.5°±5.0°. The soft restraints were removed from the refinement after sufficient convergence, as discussed below.

Data from the ±44°, ±90°, and ±145° detector banks of the SEPD instrument were simultaneously used in the structural refinement, providing data for momentum transfers ranging from 10.5 to 93.8 nm^{-1} which corresponds to Bragg reflections for d-spacings between 0.0670 and 0.598 nm. The fractional occupation of the deuterium placed at the hydrogen sites was allowed to vary, with the fractional occupation of all sites constrained to a single value to take into account imperfect deuteration of the sample. The positions of the water and hydroxyl molecules were allowed to shift, accounting for the majority of the discrepancy between the collected data and the structural model. After the position of the water and hydroxyl molecules had converged, the position of the additional heavy atoms (Ca, Al, and S) were also allowed to shift with only the aluminum atom located at (0,0,0) fixed by the choice of the unit cell origin. The isotropic atomic thermal motion parameters, U_{iso}, for all atoms were allowed to vary. The U_{iso} parameters appear in the Debye–Waller correction to the atomic scattering lengths used in the structure factor calculation and represent the mean-square displacement of an atom from its equilibrium position in the crystal lattice. The Debye–Waller correction is given by,

$$e^{-(|\vec{Q}|^2 U_{iso})/2}, \quad (1)$$

where $|\vec{Q}|$ is the magnitude of the momentum transfer vector for the scattering process.

Once the position and thermal motion parameters of all atoms had converged, the soft restraints on the hydroxyl, water, and sulfate molecules were removed and the structure was again allowed to converge. Table 1 summarizes the structural and experimental details while Table 2 contains the final fractional atomic coordinates, isotropic thermal motion parameters, and fractional occupations. Fig. 2 demonstrates the fit of the final ettringite structural model to the data from the ±145° detector banks. The overall fit is quite good with small deviations near the reflections at 0.256 nm. The fit of the revised ettringite structural model to the ±44° and ±90° detector banks is of similar quality. Table 3 summarizes the simultaneous fit of the structural model to data from the three SEPD detector banks used in the refinement. The final refinement gave an overall χ^2 of 3.951 [13] which is to be compared with an overall χ^2 of 10.21 achieved with the structural model of Berliner [4] applied to the present data. Inspection of the Berliner structural solution applied to the present data revealed that the most striking discrepancies persisted in the high momentum transfer region of the data which was only partially accessible by the diffractometer used in the prior investigation.

Table 1
Structural and experimental details

Crystal data:	
Chemical formula	$Ca_6[Al(OD)_6]_2(SO_4)_3{\cdot}25.5D_2O$
Chemical formula weight [g/mole]	1309.3
Cell setting	Trigonal
Space group	P 3 1 c
a [nm]	1.1166881 (82)
c [nm]	2.135366 (22)
Unit cell volume [nm^3]	2.3064 (3)
Z	2
Temperature [K]	10
Color	White
Crystal habit	Acicular
Data collection:	
Instrument	SEPD at IPNS, Argonne National Laboratory
Sample mounting	Vanadium can
Radiation type	Pulsed neutron
Data collection method	Time-of-flight

3.2. Ettringite structure

The positions of the calcium, aluminum, and sulfur atoms determined in this study remained essentially unchanged from the single-crystal X-ray investigation of Moore and Taylor [14]. The positions of the oxygen atoms were slightly modified from those of Moore and Taylor and the hydrogen sites were observed to be shifted relative to the structural solution due to Berliner [4]. Treatment of the hydroxyl and water molecules with soft restraints in lieu of the rigid-body constraints employed by Berliner [4] permitted greater freedom in determining the equilibrium positions of the hydrogen sites. The more precise determination of the hydrogen sites elucidated the underlying hydrogen bond network in the ettringite structure. While the positions of some atoms were shifted in the current structural refinement, relative to prior neutron and X-ray investigations, the overall structural motif of ettringite remained unchanged with a central column consisting of aluminum and calcium coordination polyhedra surrounded by columns consisting of sulfate tetrahedra and water molecules.

Fig. 3 shows a projection of the ettringite unit cell along the *c*-axis with coordination polyhedra drawn for calcium, aluminum, and sulfur to aid in visualization of the structure. O–H bonds are shown as short, black bonds (blue in the on-line version) while the hydrogen bonds are long, light grey bonds (green in the on-line version). Hydrogen bonds were deemed to be those bonds in which a hydrogen site was observed between two oxygen atoms separated by a distance of

Table 2
Fractional atomic coordinates, isotropic thermal displacement parameters, and fractional occupancy for the final ettringite structural refinement model

Atom ID	X	Y	Z	U_{iso}*100 [10^{-2} nm^2]	Fractional occupation
Al(1)	0	0	0	0.87 (19)	1.000
Al(2)	0	0	0.2500 (18)	1.45 (19)	1.000
Ca(1)	0.01728 (71)	0.81739 (67)	0.87354 (76)	0.16 (13)	1.000
Ca(2)	0.99562 (97)	0.18454 (69)	0.12035 (80)	0.53 (13)	1.000
O(1)	0.98382 (70)	0.12132 (73)	0.94179 (36)	0.018 (28)	1.000
D(1)	0.98854 (87)	0.20257 (76)	0.96238 (43)	2.17 (18)	0.9623 (30)
O(2)	0.98842 (71)	0.86144 (68)	0.04767 (38)	0.153 (28)	1.000
D(2)	1.01959 (70)	0.80734 (66)	0.03030 (37)	0.62 (13)	0.9623 (30)
O(3)	−0.00939 (80)	0.12449 (78)	0.80253 (37)	0.081 (28)	1.000
D(3)	−0.00130 (94)	0.20769 (81)	0.78399 (45)	3.04 (20)	0.9623 (30)
O(4)	0.00098 (81)	0.86182 (68)	0.18962 (33)	0.127 (28)	1.000
D(4)	0.00302 (72)	0.79409 (60)	0.21801 (32)	0.59 (11)	0.9623 (30)
O(5)	−0.01163 (99)	0.33879 (82)	0.04562 (47)	1.44 (19)	1.000
D(5a)	0.06576 (79)	0.41250 (83)	0.02238 (41)	1.83 (17)	0.9623 (30)
D(5b)	−0.08851 (86)	0.35436 (91)	0.03612 (51)	2.72 (20)	0.9623 (30)
O(6)	0.00925 (89)	0.66069 (77)	0.95641 (46)	0.64 (14)	1.000
D(6a)	−0.08154 (73)	0.58617 (75)	0.96669 (39)	1.28 (14)	0.9623 (30)
D(6b)	0.08387 (80)	0.64300 (82)	0.96162 (45)	2.19 (19)	0.9623 (30)
O(7)	0.00390 (87)	0.34609 (76)	0.20013 (45)	0.88 (16)	1.000
D(7a)	0.07465 (83)	0.40037 (86)	0.22763 (44)	3.00 (21)	0.9623 (30)
D(7b)	−0.07236 (83)	0.35908 (88)	0.21121 (46)	2.54 (20)	0.9623 (30)
O(8)	0.99670 (88)	0.65662 (73)	0.78884 (44)	0.48 (14)	1.000
D(8a)	0.91400 (82)	0.56666 (89)	0.78262 (46)	2.24 (19)	0.9623 (30)
D(8b)	1.06053 (88)	0.62622 (96)	0.78286 (51)	3.14 (16)	0.9623 (30)
O(9)	0.27089 (64)	0.40715 (66)	0.62005 (51)	0.42 (12)	1.000
D(9a)	0.28372 (113)	0.47302 (117)	0.65001 (51)	6.12 (33)	0.9623 (30)
D(9b)	0.29146 (111)	0.46375 (105)	0.57734 (44)	3.58 (21)	0.9623 (30)
O(10)	0.75483 (80)	0.60037 (86)	0.37292 (75)	2.54 (18)	1.000
D(10a)	0.70681 (110)	0.53234 (107)	0.33675 (42)	3.44 (24)	0.9623 (30)
D(10b)	0.70225 (82)	0.535754 (75)	0.40751 (35)	1.09 (13)	0.9623 (30)
O(11)	0.25358 (73)	0.41070 (80)	0.13011 (48)	1.24 (16)	1.000
D(11a)	0.31831 (79)	0.37355 (84)	0.12870 (68)	5.36 (23)	0.9623 (30)
D(11b)	0.28293 (56)	0.49551 (63)	0.10470 (35)	0.39 (10)	0.9623 (30)
O(12)	0.75758 (70)	0.58990 (76)	0.86986 (60)	1.07 (14)	1.000
D(12a)	0.70580 (68)	0.64553 (66)	0.87646 (67)	2.84 (16)	0.9623 (30)
D(12b)	0.68462 (99)	0.49216 (97)	0.85504 (51)	6.86 (31)	0.9623 (30)
O(19)	0.19655 (138)	0.62933 (154)	0.23225 (73)	0.016 (300)	0.4986 (70)
D(19a)	0.27865 (124)	0.63321 (305)	0.24555 (118)	3.11 (38)	0.4774 (70)
D(19b)	0.21255 (147)	0.72514 (170)	0.20972 (81)	2.77 (42)	0.4774 (70)
S(1)	1/3	2/3	0.48610 (127)	0.34 (18)	1.000
O(13)	1/3	2/3	0.42314 (85)	2.08 (39)	1.000
O(16)	0.19724 (78)	0.62973 (80)	0.51087 (40)	1.06 (15)	1.000
S(2)	1/3	2/3	0.75133 (63)	0.10 (18)	1.000
O(14)	1/3	2/3	0.81909 (97)	4.65 (58)	1.000
O(17)	0.19730 (82)	0.63822 (90)	0.71742 (43)	2.38 (19)	1.000
S(3)	1/3	2/3	0.00518 (148)	0.31 (18)	1.000
O(15)	1/3	2/3	0.06442 (76)	1.92 (40)	1.000
O(18)	0.18695 (78)	0.56856 (76)	−0.01993 (40)	0.69 (14)	1.000

less than 0.330 nm. Coordination polyhedra and bonds for those structures lying at the edges of the unit cell are incomplete and thus are omitted when the structure is visualized. As discussed by Moore and Taylor [14], the aluminum atoms are six-fold coordinated with hydroxyls while the calcium atoms are each eight-fold coordinated with four hydroxyls and four water molecules. The hydroxyls are observed to hydrogen bond to water molecules located on the calcium coordination polyhedron on the opposite side of a shared aluminum coordination polyhedron. The hydrogen bonds formed by the hydroxyls add some measure of structural support for the column consisting of calcium and aluminum coordination polyhedra. Water molecules on the calcium coordination polyhedra are observed to form hydrogen bonds with other calcium coordination polyhedra as well as with the columns of sulfate tetrahedra and water molecules. Those water molecules located on the same equatorial plane as the calcium atoms have an alternating pattern with one water molecule having a nearly horizontal arrangement, forming a hydrogen bond with an adjoining calcium coordination polyhedron and a second hydrogen bond with a nearby column of sulfate tetrahedra and water molecules. The next water molecule has

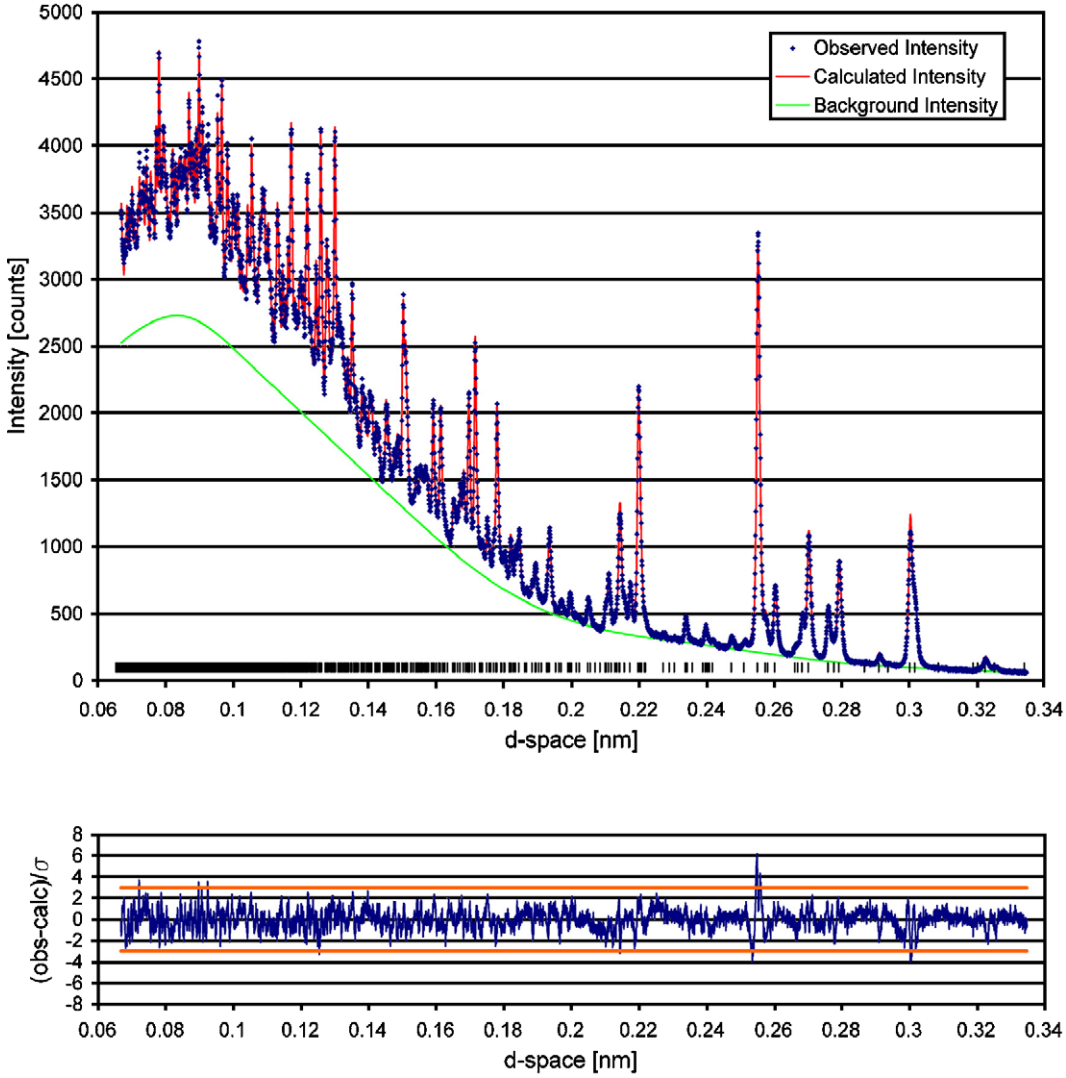

Fig. 2. Fit of the refined ettringite structural model to the data from the ±145° detector banks of the SEPD instrument with reflection locations indicated by vertical tick marks (above). The error in the structural model is also shown with solid orange lines at ±3 standard deviations (below).

a more vertical arrangement and is hydrogen bonded exclusively to a nearby column of sulfate tetrahedra and water molecules. Those water molecules that do not lie on the same equatorial plane as the calcium atoms are observed to hydrogen bond with adjacent columns of sulfate tetrahedra and water

Table 3
Summary of the fit of the ettringite structural model to various SEPD detector banks

Detector bank	R_p	R_{wp}	Number of observed reflections
±44°	0.0151	0.0195	829
±90°	0.0190	0.0265	2838
±145°	0.0197	0.0272	3963

$$R_p \equiv \frac{\sum |I_{Observed} - I_{Calculated}|}{\sum I_{Observed}}$$

$$R_{wp} \equiv \left(\frac{\sum w(I_{Observed} - I_{Calculated})^2}{\sum w I^2_{Observed}} \right)^{1/2}$$

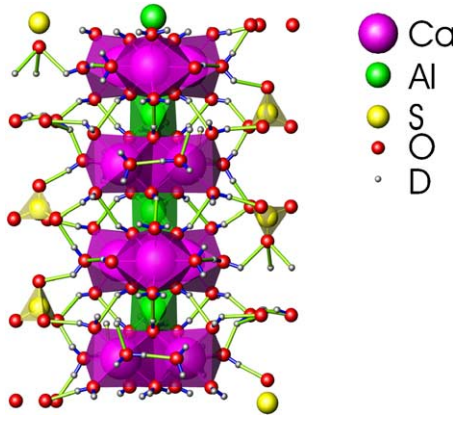

Fig. 3. A projection of the ettringite crystal structure along the *c*-axis illustrating the hydrogen bonding network along the central column of calcium and aluminum coordination polyhedra.

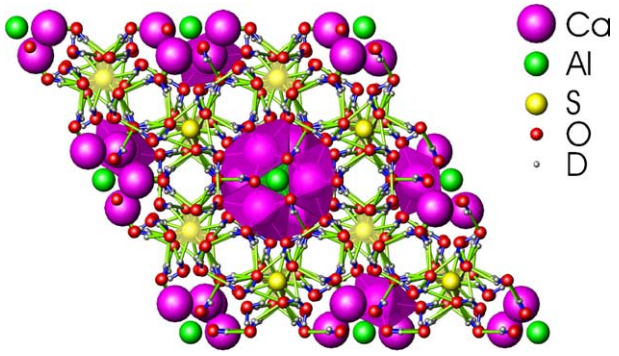

Fig. 4. 2 × 2 × 2 ettringite unit cell configuration as viewed down the *c*-axis demonstrating the extensive hydrogen bonding between columns.

molecules. Fig. 4 shows a view down the *c*-axis for a 2 × 2 × 2 unit cell configuration of ettringite. Focusing on the column composed of aluminum and calcium coordination polyhedra located at the center of Fig. 4, the extensive hydrogen bonding of the water molecules associated with the calcium coordination polyhedra with the six surrounding columns of sulfate tetrahedra and water molecules is evidenced by the large number of hydrogen bonds emanating from the central column.

The hydrogen bond network within ettringite is complete with all hydrogen sites participating in it. The distances and angles associated with the hydrogen bond network are detailed in Table 4 (Note: entries in Table 4 are listed as O–D and O–D––O to emphasize that the actual material was deuterated). The observed hydrogen bond distances (O––H) ranging from 0.1708 to 0.2347 nm and hydrogen bond angles (O–H––O) ranging from 110.6° to 173.1° are typical of other hydrogen bond networks [15,16]. On average, the hydroxyls were observed to have an O–H bond length of 0.0962 nm, an H––O bond length of 0.2263 nm, and an O–H––O angle of 158.7°. The water molecules were observed to have, on average, an O–H bond length of 0.0987 nm, an H––O bond length of 0.1919 nm, and an O–H––O angle of 153.1°. The hydrogen bond network clearly plays an important role in stabilizing the ettringite structure and provides a connective framework for the columnar structure.

The final fractional occupation of deuterium on the hydrogen sites suggests an effective deuteration of the hydrogen sites of 99.76%, a reasonable value given that the certificate of analysis for the D_2O used in the direct-synthesis method stated a deuterium fraction of 99.9%. The occupancy of the channel water site, as determined by the occupation of O(19), D(19a), and D(19b), infers a chemical formula for the ettringite studied of $Ca_6[Al(OD)_6]_2(SO_4)_3 \cdot 25.5D_2O$.

Table 4
Summary of ettringite hydrogen bond network

Description	Distance [nm]	Angle [°]	Description	Distance [nm]	Angle [°]
Hydroxyls:					
O(1)–D(1)	0.0986		O(2)–D(2)	0.0913	
O(1)–D(1)––O(5)	0.2340	156.9	O(2)–D(2)––O(6)	0.2235	151.0
O(3)–D(3)	0.0972		O(4)–D(4)	0.0978	
O(3)–D(3)––O(7)	0.2347	153.9	O(4)–D(4)––O(8)	0.2130	173.0
Water molecules:					
O(5)–D(5a)	0.0979		O(6)–D(6a)	0.0962	
O(5)–D(5b)	0.0979		O(6)–D(6b)	0.0954	
D(5a)–O(5)–D(5b)		103.3	D(6a)–O(6)–D(6b)		116.5
O(5)–D(5a)––O(18)	0.1824	167.3	O(6)–D(6a)––O(16)	0.1813	151.9
O(5)–D(5b)––O(16)	0.1894	164.3	O(6)–D(6b)––O(18)	0.1769	164.6
O(7)–D(7a)	0.0926		O(8)–D(8a)	0.0976	
O(7)–D(7b)	0.0962		O(8)–D(8b)	0.0939	
D(7a)–O(7)–D(7b)		106.0	D(8a)–O(8)–D(8b)		96.2
O(7)–D(7a)––O(19)	0.2218	127.9	O(8)–D(8a)––O(19)	0.1752	149.6
O(7)–D(7b)––O(17)	0.2019	161.6	O(8)–D(8b)––O(17)	0.2025	138.9
O(9)–D(9a)	0.0930		O(10)–D(10a)	0.1027	
O(9)–D(9b)	0.1067		O(10)–D(10b)	0.0985	
D(9a)–O(9)–D(9b)		102.5	D(10a)–O(10)–D(10b)		97.6
O(9)–D(9a)––O(17)	0.1708	149.1	O(10)–D(10a)––O(14)	0.1890	173.3
O(9)–D(9b)––O(16)	0.1764	164.9	O(10)–D(10b)––O(18)	0.2014	146.0
O(11)–D(11a)	0.0998		O(12)–D(12a)	0.1049	
O(11)–D(11b)	0.0994		O(12)–D(12b)	0.1033	
D(11a)–O(11)–D(11b)		114.7	D(12a)–O(12)–D(12b)		106.9
O(11)–D(11a)––O(9)	0.1863	168.1	O(12)–D(12a)––O(10)	0.2078	170.2
O(11)–D(11b)––O(15)	0.1906	173.1	O(12)–D(12b)––O(13)	0.2223	110.6
O(19)–D(19a)	0.0940				
O(19)–D(19b)	0.1103				
D(19a)–O(19)–D(19b)		113.9			
O(19)–D(19a)––O(19)	0.1840	112.8			
O(19)–D(19b)––O(11)	0.1865	128.2			

Note: Chemical bonds are denoted with a single dash (–) while hydrogen bonds are denoted with a double dash (––).

4. Conclusion

The ettringite crystalline structure has been investigated using TOF neutron powder diffraction techniques in combination with the Rietveld crystal structure refinement method. The resultant ettringite structure has heavy atom positions very similar to previous single-crystal X-ray investigations but with well determined hydrogen atomic site locations. The precise determination of the hydrogen atomic sites permits a detailed understanding of the hydrogen bonding network within the ettringite structure. The revised structural model permits more accurate identification of ettringite in multi-phase mixtures and will be incorporated into the analysis of investigations, currently underway, of ettringite formation and thermal decomposition using TOF neutron diffraction techniques.

Acknowledgements

This work has benefited from the use of the Intense Pulsed Neutron Source (IPNS) at Argonne National Laboratory. IPNS is funded by the U.S. Department of Energy, BES-Materials Science, under Contract W-31-109-ENG-38. Funding for this work was provided in part by National Science Foundation Grant CMS-0196400. The authors would also like to thank Professor Michael Atzmon for his thoughtful comments on the preparation of this manuscript.

References

[1] H.F.W. Taylor, Cement Chemistry, 2nd edn, Thomas Telford, London, 1997.
[2] M. Santhanam, M.D. Cohen, J. Olek, Sulfate attack research-whither now? Cem. Concr. Res. 31 (2001) 845–851.
[3] H.F.W. Taylor, C. Famy, K.L. Scrivener, Delayed ettringite formation, Cem. Concr. Res. 31 (2001) 683–693.
[4] R. Berliner, The structure of ettringite, in: Menashi Cohen, Sidney Mindess, Jan Skalny (Eds.), Materials Science of Concrete, The Sidney Diamond Symposium, The American Ceramic Society, Westerville, OH, 1998, pp. 127–141.
[5] M.R. Hartman, R. Berliner, J. Solid State Chem. (in press).
[6] L.J. Struble, P.W. Brown, An Evaluation of Ettringite and Related Compounds for Use in Solar Energy Storage, NBSIR 84-2942, U.S. Department of Commerce, National Bureau of Standards, Gaithersburg, MD, 1984.
[7] H. Pöllmann, H.-J. Kuzel, R. Wenda, Compounds with ettringite structure, N. Jb. Miner. Abh. 160 (1989) 133–158.
[8] J.D. Jorgensen, J. Faber, J.M. Carpenter, R.K. Crawford, J.R. Haumann, R.L. Hitterman, R. Kleb, G.E. Ostrowski, F.J. Rotella, T.G. Worlton, Electronically focused time-of-flight powder diffractometers at the intense pulsed neutron source, J. Appl. Crystallogr. 22 (1989) 321–333.
[9] H.M. Rietveld, A profile refinement method for nuclear and magnetic structures, J. Appl. Crystallogr. 2 (1969) 65–71.
[10] A.C. Larson, R.B. Von Dreele, General Structure Analysis System (GSAS), Los Alamos National Laboratory Report LAUR 86-748, 2000.
[11] B.H. Toby, EXPGUI, a graphical user interface for GSAS, J. Appl. Crystallogr. 34 (2001) 210–213.
[12] R.A. Young (Ed.), The Rietveld Method, Oxford University Press, Oxford, 1993.
[13] $\chi^2 \equiv \frac{\sum w(I_{\text{observed}} - I_{\text{Calculated}})^2}{(N_{\text{observations}} - N_{\text{Variables}})}$.
[14] A.E. Moore, H.F.W. Taylor, Crystal structure of ettringite, Acta Crystallogr., B 26 (1970) 386–393.
[15] G.A. Jeffrey, An Introduction to Hydrogen Bonding, Oxford University Press, New York, 1997.
[16] M. Falk, O. Knop, Water in stoichiometric hydrates, in: F. Franks (Ed.), Water, A Comprehensive Treatise, vol. II, Plenum Press, New York, 1973, pp. 55–113.